Influence of nodular defects on the laser damage resistance of optical coatings in the femtosecond regime

Laurent Gallais,[1,*] Xinbin Cheng,[2,3] and Zhanshan Wang[2,3]

[1]*Institut Fresnel, Aix-Marseille Université, CNRS, Ecole Centrale Marseille, Campus de St Jérôme, 13013 Marseille, France*

[2]*MOE Key Laboratory of Advanced Micro-Structured Materials, Shanghai 200092, China*

[3]*Institute of Precision Optical Engineering, School of Physics Science and Engineering, Tongji University, Shanghai 200092, China*

**Corresponding author: laurent.gallais@fresnel.fr*

Received January 9, 2014; accepted January 25, 2014;
posted February 10, 2014 (Doc. ID 203850); published March 12, 2014

The influence of nodular coating defects on the sub-picosecond laser damage resistance of multilayer coatings is investigated. The study is conducted on engineered nodules from monodisperse silica microspheres in HfO_2/SiO_2 high-reflective mirrors, at 400 fs/1030 nm. We demonstrate through an experimental study coupled with 3D finite-difference time-domain simulations that nodules in dielectric multilayer coatings are a main concern for the damage resistance of femtosecond optics. The nodules, and hence possibly other defects that produce E-field enhancement in coating materials, induce damage initiation at very low fluences (0.1 J/cm^2 in the case under study) compared to the intrinsic damage threshold of the component (1.4 J/cm^2 for the present mirror). After initiation, the damage sites grow catastrophically at a determined threshold, reducing significantly the damage resistance (0.6 J/cm^2) but allowing a "safe" operating fluence to be defined.

OCIS codes: (140.3330) Laser damage; (140.7090) Ultrafast lasers; (310.0310) Thin films.
http://dx.doi.org/10.1364/OL.39.001545

Laser damage resistance of optical components is a main concern for high power femtosecond laser and applications. Particularly, the laser-induced damage threshold (LIDT) of optical coatings inhibits the available power and long-term resistance of short pulse laser systems. To design and manufacture such components it is critical to know the power handling capability of the materials and, for that purpose, to study the LIDT of single layer or multilayer coatings. From experimental studies, the dependence of the LIDT with the material properties (bandgap, refractive index) have been identified [1,2] and applied to design multilayer coatings with enhanced damage resistance [3–5]. Because damage process in the sub-picosecond regime is the result of the coupling of energy in the material by nonlinear absorption mechanisms, a highly deterministic LIDT is typical. This has been evidenced experimentally on different optical materials [6–8]. Therefore, if the damage resistance of a material is directly related to the intensity, any local enhancement of the E-field should decrease the LIDT. This is, for example, observed on gratings where the damage threshold is directly related to the intensity in the pillars of the structure [9,10]. In the case of dielectric coatings, nodular defects, which are macroscopic defects embedded in the structure [11], can induce such local intensity enhancement. As a consequence they are the main limitation for the laser damage resistance of large optics in the nanosecond regime [12]. Depending on the nodule geometry, stack design, wavelength, angle of incidence, and based on numerical simulations, the light intensification can reach a factor greater than 10 as compared to the maximum value in the multilayer stack [13,14]. Consequently, one should expect a significant decrease of the LIDT of the nodular sites under femtosecond irradiation. However, such effects have not been studied up to now in this regime. Therefore, we have conducted a specific study of this topic in order to state if such nodular defects are an issue for the laser damage resistance of optical coatings. The questions we have tried to answer in the present Letter are: do nodular sites initiate damage at very low fluences compared to the intrinsic damage threshold and, if that is the case, do the damaged sites grow under successive and low fluence irradiations?

Our work is based on the analysis of the behavior of artificial nodular defects in high-reflective (HR) mirrors in order to obtain a large amount of identical and perfectly characterized nodular sites to conduct statistical studies. Such an approach is indeed very useful for understanding pathways leading to laser damage of thin films [15]. For that purpose, we used monodisperse silica microspheres deposited on the surface of a BK7 subtrate. A HfO_2/SiO_2 HR coating working for normal incidence at 1064 nm was deposited on top of the substrate {design: [Glass: $(HL)^{13}$L: Air]}. A HR coating on a clean substrate (i.e., without silica microspheres), as silica and hafnia single layers (SL), were also manufactured and studied in order to compare the LIDT values. A detailed description of the manufacturing and characterization of the samples used in the present study can be found in [14]. The sizes of the microspheres were chosen to be 1.9 μm in diameter in order to obtain a strong E-field enhancement [14] and evidence the potential effect of the nodules. The $|E^2|$ distributions were simulated using a 3D finite-difference time-domain (FDTD) electromagnetic code described in [14]. The current simulation has two differences compared to previous simulations. The first is that the simulation domain is bigger and the resolution of gridding cells is also improved. It is worth noting that the recalculation of E-field enhancement at 1064 nm using the current simulation domain gives the peak $|E^2|$ value of 24. Previous results tend to underestimate the light intensification. The second is that a plane wave with a center wavelength of 1030 nm is used as the incident field. For this nodular geometry, the E-field enhancement

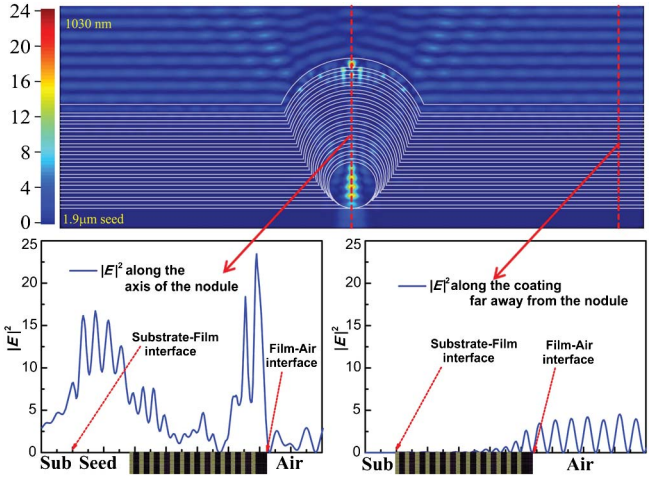

Fig. 1. FDTD-simulated $|E^2|$ distributions for the nodule under consideration. The white lines represent film interfaces. The refractive indexes used in simulations were 1.45 for silica (coating, substrate, and microsphere) and 1.96 for hafnia.

should be smaller at 1030 nm than at 1064 nm, because the incident angular range is larger at 1030 nm than at 1064 nm. Fig. 1 shows the results of simulations for the geometry under consideration. The results are compared to the case of the HR coating free of nodule.

The $|E^2|$ enhancement in the seed of the nodule is still very strong (16 times), which is similar to the case of $|E^2|$ enhancement at 1064 nm. Additionally, a strong $|E^2|$ enhancement (23 times) is also created at the top silica layer. The mechanisms, such as resonant effect, surface modes, etc., are still under investigation to explain why the highest $|E^2|$ is localized in the top silica layer. We can note, however, that the geometry of the nodule is not perfectly known; therefore, introducing small changes in geometry should change the highest $|E^2|$ value, and only the order of magnitude is significant. In the case of the perfect HR coating, a ratio of 1.96 in silica and 1.11 in hafnia are obtained, and the maxima are localized at the entrance of the stack.

The laser damage studies of the samples were conducted on the experimental setup described in [8]. The test conditions were: 1030 nm wavelength, 350 fs ± 20 fs pulse duration estimated from single shot autocorrelation trace and sech fit, and Gaussian spatial profile in the location of the sample plane with a 30 μm radius at 1/e. For the single layers and the "perfect" HR coating we have tested the sample with a S-on-1 procedure, with S from 1 to 10^4, at 10 Hz or 1 kHz, and random sites were chosen for statistical tests. Damage was defined as any visible modification observed with the in-line Nomarksi microscope in the damage testing system.

In the case of the HR coating with nodules, the test procedure was to individually irradiate sites with nodules. For that purpose, the sample is moved in a defined test area until a nodule is observed under the in-line microscope. The sample is then finely moved in order to align the nodule with the beam center. We can estimate the pointing accuracy to be ±2 μm, resulting in a relative fluence error of less than 1% at the position of the nodule. Taking into account the shot to shot variations of the laser, the relative error budget was less than 3% for

Table 1. Measured LIDT of SL and HR Nodule Free Coatings (Fluence Error Bars are within ±0.03 J/cm²)

	Measured			Calculated
	LIDT (J/cm²)			LIDT (J/cm²)[a]
Shots	HfO_2 SL	SiO_2 SL	HR	HR
1	1.72[b]	2.03[b]	1.57	1.55
10	1.68[b]	1.97[b]	1.48	1.51
10^2	1.57[b]	1.97[b]	1.44	1.41
10^3	1.60[b]	1.97[b]	1.44	1.44
10^4	1.51[b]	1.93[b]	1.47	1.36

[a]The last column is the theoretical LIDT of the HR coating based on its design and on the LIDT of SL films.
[b]Internal fluence.

comparison of nodular sites. The laser beam is set to a test fluence and a defined number of shots is applied (from 1 to 10^4 at 10 Hz or 1 kHz). Each test procedure is applied on different nodules (typically 5) to have some statistical data. In total, the results that will be shown and discussed below have been obtained by testing more than 200 different nodule sites.

The LIDT values measured on the SL and HR coatings are given in Table 1. For the SL we give the "internal" LIDT as defined in [2], i.e., the measured LIDT corrected by taking into account the E-field distribution in the film.

A decrease of the LIDT with the number of shots is observed on the 3 tested samples. This effect is explained with the accumulation of electronic defects in the materials [16]. For the HR coatings, the decrease of LIDT is less than 10% after 10,000 successive shots. From the measured LIDT of the SL, one can calculate the theoretical LIDT of the HR coating by calculating the E-field distribution in the stack and divide the highest $|E^2|$ by the internal LIDT of the materials [17]. With the HR design under consideration, HfO_2 is the material that limits the LIDT. Measured and calculated values are close to each other, which indicates that the LIDT of the HR is related to the upper HfO_2 film (second layer of the stack) and that the fatigue effect of HfO_2 is the same in air and in the multilayer stack.

In the case of nodules, a summary of the experimental results is given in Fig. 2 which can be qualitatively described as follows:

- For very low fluences (up to ≈0.1 J/cm²) we have not observed any modifications by Nomarski microscopy nor SEM.
- For fluences between ≈0.1 J/cm² to ≈ 0.3 J/cm² a modification of the nodule was detected by the image analysis algorithm used for damage detection. However, no ejection of the nodule has occured and the site is stable under multiple irradiation. Depending on the fluence, this effect can occur after 1 or several hundreds of shots (cross symbol on the figure).
- For fluences between ≈0.3 J/cm² to ≈0.65 J/cm² we have observed an ejection of the nodule after 1 shot, without growth after multiple irradiations.
- At higher fluences, however, the ejected nodule area is not stable anymore after multiple irradiations. Depending on the fluence the growth speed is different, but the

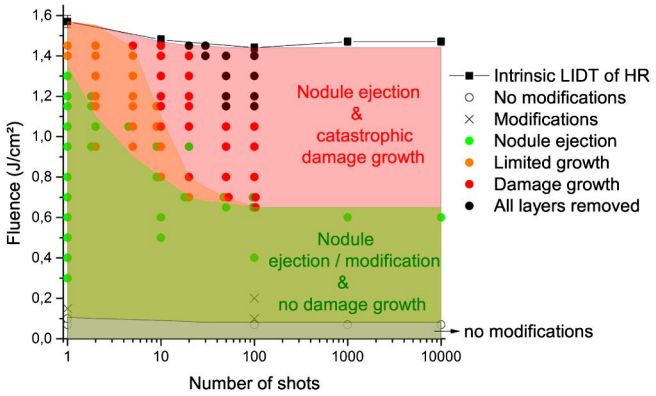

Fig. 2. Results of multiple irradiations on individual nodular sites. Each point corresponds to several investigated nodules (1–5). When two points are plotted for a given irradiation sequence it means that different situations have been observed. "*No modification*": nothing visible under Nomarski microscope; "*Modification*": a change has been observed but the nodule is not ejected; "*Nodule ejection*": nodule has been ejected without extended damage (situation 1 in Fig. 3); "*Limited growth*": nodule has been ejected and collateral damage area is limited to less than 2 times the initial nodule area (situation 2 in Fig. 3); "*Damage growth*": nodule has been ejected with extended damage (situation 5 in Fig. 3); "*All layers removed*": nodule has been ejected and damage has grown up to the point that all layers of the coating have been removed (situation 50 in Fig. 3).

damage always grows catastrophically, up to the point where all layers are removed (example in Fig. 3).

The different situations described above are shown on Fig. 2, with color areas as guides to the eye. The typical damage morphologies that we have observed are given in Fig. 3.

These experimental results show evidence that nodules drastically reduce the damage threshold. In the present case, the highest $|E^2|$ is located in the silica microsphere and in the silica overcoat of the stack. If we consider that the internal LIDT of the silica microsphere is the same as the measured silica coating ($\approx$2 J/cm^2) and taking into account the ratio of 23 and 16 previously calculated (ratio of the maximum $|E^2|$ localized in the silica overcoat and in the seed of the nodule) one finds an incident fluence between 0.12 J/cm^2 and 0.09 J/cm^2 to initiate damage. This value is in good agreement with the experimental one; modifications have been observed starting from 0.15 J/cm^2 and nothing has been observed below 0.1 J/cm^2.

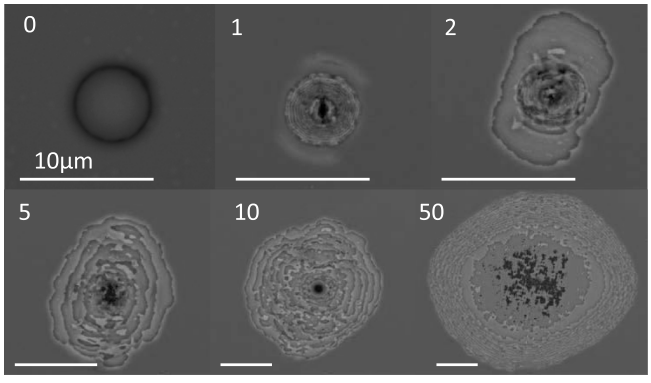

Fig. 3. Damage growth at the nodular sites under successive irradiations at 1.45 J/cm^2. Each SEM image corresponds to a different site on the sample.

Even though the initiation mechanism in the nodule can be understood and predicted with simulations, the damage growth mechanism is, however, much more complex and cannot be predicted with our current knowledge. The study of the physical mechanisms responsible for this growth is out of the scope of this Letter; however, we can distinguish 2 main contributions to this effect. The first one is a modification of the materials under heating and plasma formation near the damaged nodule area. The created electronic defects will induce a more efficient coupling of laser energy in the surrounding area and, as a result, this area will be damaged at lower fluences than the pristine materials. The second one could be linked to mechanical effects; when the nodule is ejected, or when a laser damage occurs, the shock wave could delaminate the films. For instance, it can be seen on the SEM images that the films at the edges of the damaged areas are no longer attached to the coating. In the part where there is a thin air layer between the delaminated film and the rest of the coating the $|E^2|$ is modified and amplified in the bottom layers, resulting in a lower damage resistance. This effect can be easily shown with simple calculations of the E-field in multilayer stacks.

As a conclusion, we have demonstrated that nodules, and potentially any macroscopic defect that can modify the E-field distribution, are a main concern for ultrashort laser optics. They induce damage initiation (nodule ejection) at very low fluence, this initiation fluence being predictable and related to the E-field enhancement and its localization. When initiated, the damage can then grow catastrophically at fluences very low compared to the intrinsic damage threshold. Following this work, further experiments should be dedicated to the study of different nodule geometries and to the investigation of damage growth mechanisms.

References

1. M. Mero, J. Liu, W. Rudolph, D. Ristau, and K. Starke, Phys. Rev. B **71**, 115109 (2005).
2. B. Mangote, L. Gallais, M. Commandré, M. Mende, L. Jensen, H. Ehlers, M. Jupé, D. Ristau, A. Melninkaitis, J. Mirauskas, V. Sirutkaitis, S. Kicas, T. Tolenis, and R. Drazdys, Opt. Lett. **37**, 1478 (2012).
3. M. Jupé, M. Lappschies, L. Jensen, K. Starke, and D. Ristau, Proc. Soc. Photo-Opt. Instrum. Eng. **6403**, 64031A (2007).
4. I. B. Angelova, A. Von Conta, S. A. Trushin, Z. Major, S. Karsch, F. Krausz, and V. Pervak, Proc. Soc. Photo-Opt. Instrum. Eng. **8190**, 81900B (2011).
5. A. Hervy, L. Gallais, D. Mouricaud, and G. Chériaux, in *Optical Interference Coatings*, OSA Technical Digest (Optical Society of America, 2013), p. FA.4.
6. A. P. Joglekar, H. Liu, G. J. Spooner, E. Meyhofer, G. Mourou, and A. J. Hunt, Appl. Phys. B **77**, 25 (2003).
7. N. Sanner, O. Utéza, B. Chimier, M. Sentis, P. Lassonde, F. Légaré, and J. C. Kieffer, Appl. Phys. Lett. **96**, 071111 (2010).
8. B. Mangote, L. Gallais, M. Zerrad, F. Lemarchand, L. H. Gao, M. Commandré, and M. Lequime, Rev. Sci. Instrum. **83**, 013109 (2012).

9. J. Neauport, E. Lavastre, G. Razé, G. Dupuy, N. Bonod, M. Balas, G. de Villele, J. Flamand, S. Kaladgew, and F. Desserouer, Opt. Express **15**, 12508 (2007).
10. J. A. Britten, W. Molander, A. M. Komashkoa, and C. P. J. Barty, Proc. Soc. Photo-Opt. Instrum. Eng. **5273**, 1 (2004).
11. H. H. Guenther, Appl. Opt. **20**, 1034 (1981).
12. M. R. Kozlowski, in *Thin Films for Optical Systems*, F. R. Flory, ed. (Marcel Dekker, 1995), pp. 521–549.
13. C. J. Stolz, S. Hafeman, and T. V. Pistor, Appl. Opt. **47**, C162 (2008).
14. X. Cheng, J. Zhang, T. Ding, Z. Wei, H. Li, and Z. Wang, Light Sci. Appl. **2**, e80 (2013).
15. S. Papernov and A. W. Schmid, J. Appl. Phys. **92**, 5720 (2002).
16. M. Mero, B. Clapp, J. C. Jasapara, W. Rudolph, D. Ristau, K. Starke, J. Kruger, S. Martin, and W. Kautek, Opt. Eng. **44**, 051107 (2005).
17. M. Jupé, M. Lappschies, L. Jensen, K. Starke, and D. Ristau, Proc. Soc. Photo-Opt. Instrum. Eng. **6720**, 6700U (2007).